Proton decay matrix elements on lattice

Jun-Sik Yoo [1]

[1]Department of Physics and Astronomy

Stony Brook University

2019 Lattice Workshop for

US-Japan Intensity Frontier Incubation, BNL,

March 25-27, 2019

Introduction

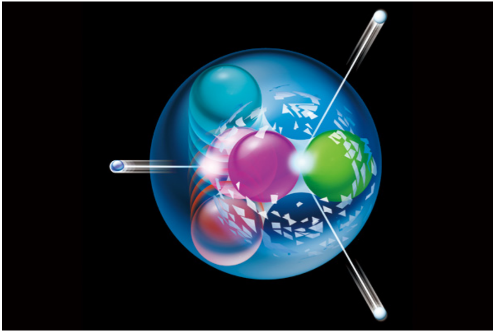

Figure 1: Proton decay image from (HYPER-K,)

$$p \longrightarrow \Pi + \bar{\ell}$$

Introduction

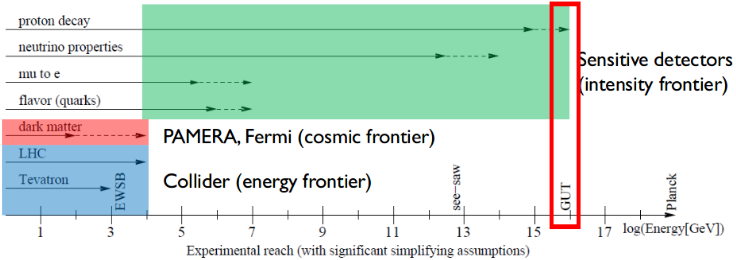

Figure 2: Energy scale of search, Zoltan Ligeti

Baryon asymmetry

Nonzero net baryon number

$\frac{n_B - \bar{n}_B}{n_\gamma} \sim 10^{-10}$

Sakharov's conditions

- At least one B violating process
- C- and CP-violation
- interactions outside of thermal equilibrium

GUT, SUSY-GUT

GUT

Symmetry group to be $G \supset SU(3)_C \otimes SU(2)_L \otimes U(1)_Y$

- Gauge problem
- Charge quantization problem
- Coupling unification
- Baryon asymmetry

SUSY-GUT

- Superpartners to particles
- Better unification at higher scale

GUT,SUSY-GUT

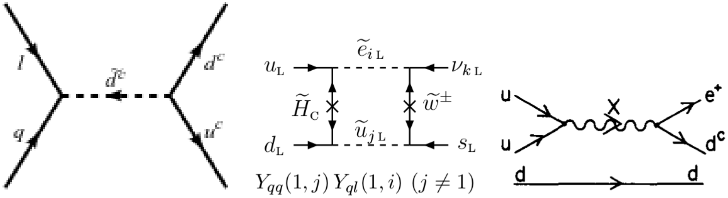

(a) d=4 operator (b) d=5 operator (c) d=6 operator

Figure 3: Possible BV operators in (SUSY-)GUT

GUT,SUSY-GUT

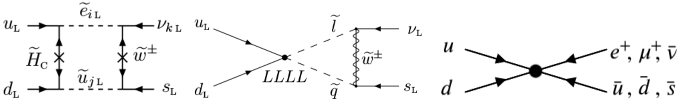

(a) $\sim \Lambda_{GUT}$ (b) $\sim \Lambda_{SUSY}$ (c) $\sim \Lambda_{EW}$

Figure 4: Proton decay operator at different scales

Model parameters come into Wilson coefficients

(a) $Y_{qq}, Y_{ql}, Y_{ud}, Y_{ue}$

(b) M_{H_C}

(c) $m_{\tilde{l}}, m_{\tilde{q}}$, triangle loop integrals, ...

Effective operators

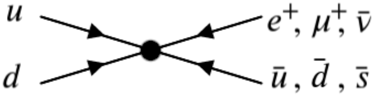

Figure 5: Four-fermion effective operators

Effective operator : $\mathcal{O}_{\Gamma\Gamma'} = (qq)_\Gamma (q\ell)_{\Gamma'}$,

$(XY)_\Gamma = (X^T \mathcal{C} P_\Gamma Y)$ $\quad$ $\mathcal{C} :=$ (Charge Conjugation Matrix)

$\langle \Pi \bar{\ell} | p \rangle_{GUT} \sim C^{\Gamma\Gamma} \langle \Pi \bar{\ell} | \mathcal{O}_{\Gamma\Gamma'} | p \rangle_{SM} = C^{\Gamma\Gamma} \bar{v}_\ell \langle \Pi | (qq)_\Gamma P_{\Gamma'} q | p \rangle$,

where $C^{\Gamma\Gamma'}$ is a wilson coefficient, Π is a meson, and p is a proton.

Decay rate

The decay rate Γ is calculated from the hadronic matrix element,

$$\begin{aligned}&\langle \Pi(p')|O^{\Gamma\Gamma'}(q)|N(p,s)\rangle\\&= \bar{v}_\ell P_{\Gamma'}\left[W_0^{\Gamma\Gamma'}(q^2) - \frac{i\not{q}}{m_N}W_1^{\Gamma\Gamma'}(q^2)\right]u_N(p,s)\\&= \bar{v}_\ell P_{\Gamma'}W_0^{\Gamma\Gamma'}(q^2)u_N(p,s) + O(m_l/m_N)\bar{v}_\ell u_N(p,s)\end{aligned} \tag{1}$$

where Π a meson, N a nucleon, and $W_{0,1}$ decay form factor(AOKI et al., 2000). Then the decay rate is

$$\Gamma\left(p \to \Pi + \bar{\ell}\right) = \frac{(m_p^2 - m_\Pi^2)^2}{32\pi m_p^3}\left|\sum_I C_I W_0^I\left(p \to \Pi + \bar{\ell}\right)\right|^2. \tag{2}$$

Experimental bound

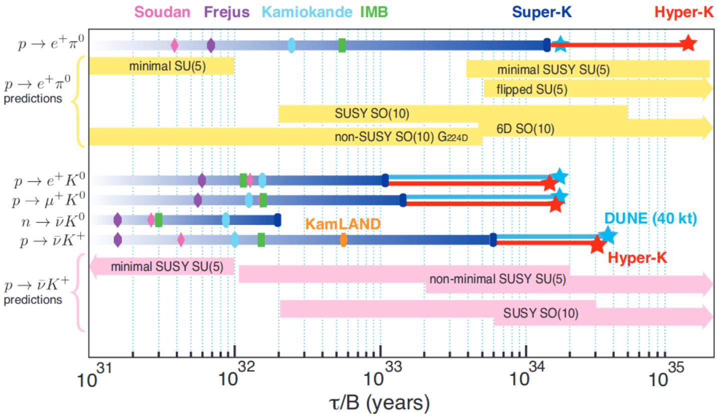

Figure 6: Current proton decay bound in SK, (ABE et al., 2018)

Lattice QCD

Formulate a strongly interacting theory on a finite, discrete euclidean spacetime $\rightarrow$ Lattice QCD

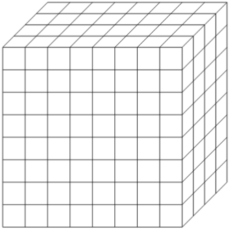

Figure 7: 3D lattice

Numerically compute observables via importance sampling

$$\langle \mathcal{O} \rangle = \frac{1}{Z} \int \mathcal{D}[\Phi] e^{-S_E[\Phi]} \mathcal{O}[\Phi]$$

$$= \frac{1}{N} \sum_{k=1}^{N} \mathcal{O}(\Phi_k)$$

- fully nonperturbative predictions from first principle
- fully gauge invariant

Stony Brook University

Matrix elements

3pt-function

(Meson)-(Decay Operator)-(Proton)

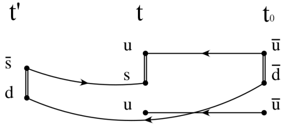

Figure 8: 3pt function, Y.Aoki

$$C^{3pt}(t,t') = \sum_{\vec{x},\vec{x}'} e^{-i\vec{q}\cdot\vec{x}} e^{i\vec{p}'\cdot\vec{x}'} \langle 0 | J_\Pi(x') \mathcal{O}(x) \bar{J}_N(x_0) | 0 \rangle$$

$$= \frac{C_\Pi^{2pt}(t'-t,\vec{p}')}{\sqrt{Z_\Pi}} \frac{\mathrm{Tr}[P C_p^{2pt}(t,\vec{p})]}{\sqrt{Z_p}} \times \langle \Pi(\vec{p}') | \mathcal{O} | N(\vec{p}) \rangle \bar{u}_N(\vec{p})$$

Matrix elements

Define the ratio $R_3(t,t') = \frac{C^{3pt}(t,t')}{C_\Pi^{2pt}(t'-t,\vec{p}')\mathrm{Tr}[PC_p^{2pt}(t,\vec{p})]}\sqrt{Z_\Pi}\sqrt{Z_p}$.
As $t \to \infty$, $R_3(t,t') \to \langle \Pi(p')|O^{\Gamma\Gamma'}(q)|N(p,s)\rangle$, giving decay form factors $W_{0,1}(q^2)$

$$\mathrm{Tr}[R_3 P_L P_4] = W_0^{\Gamma L}(q^2) - \frac{iq_4}{m_N} W_1^{\Gamma L}(q^2).$$

$$\mathrm{Tr}[R_3 P_L i P_4 \gamma_j] = \frac{q_j}{m_N} W_1^{\Gamma L}(q^2)$$

Momentum transfer is chosen to be $q^2 \sim 0$: $\vec{p} = \vec{q} + \vec{p}'$

Stony Brook University

Matrix elements

2pt correlation function

Ex) Kaon

Interpolating operator for Kaon : $J_{K^+}(x) = \bar{s}(x)\gamma_5 u(x)$.

$$C_K^{2pt}(t,\vec{p}) = \sum_{\vec{x}} e^{i\vec{p}\cdot\vec{x}} \langle 0|J_K(t,\vec{x})J_K^\dagger(0,\vec{0})|0\rangle$$
$$= \frac{Z_K}{2E(\vec{p})} e^{-E(\vec{p})t}$$

where $\sqrt{Z_K} = \langle 0|J_K|K\rangle$

Identity matrix used is: $\mathbb{1} = \sum_{\vec{p}} |K;\vec{p}\rangle \frac{1}{2E(\vec{p})} \langle K;\vec{p}| + \ldots$

Matrix elements

2pt correlation function

Ex) Kaon

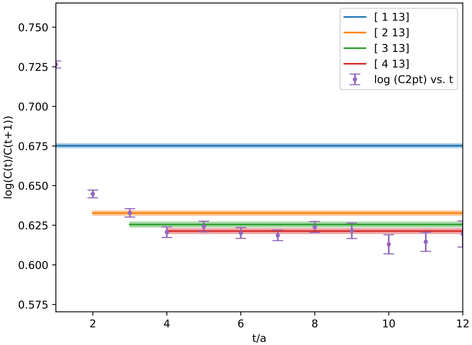

Figure 9: Kaon 2pt function with momentum [0 1 1] in log plot

Lattice settings

RBC/UKQCD generated $N_f = 2+1$ dynamic Domain wall Fermion, gauge action Iwasaki-DSDR

Lattice size $24^3 \times 64 (L \sim 4.8 fm)$, $L_5 = 24$,

$\beta = 1.633$, $m_\ell a = 0.00107$, $m_h a = 0.0850$, $m_{res} = 0.00228$

$a^{-1} = 1.0$ GeV, $m_\pi a = 139$, $m_K a = 505$, $m_\pi L \sim 3.4$

Deflated CG with 2000 Eigenvectors (basis 1000)

Generated 32+1 AMA samples on 102 gauge configurations with 3 source-sink separation, i.e., $t_{sep} \in \{8, 9, 10\}$

To meet the kinematic condition, chose the most suitable two sets of $\vec{p}$ for each meson.

Matrix elements

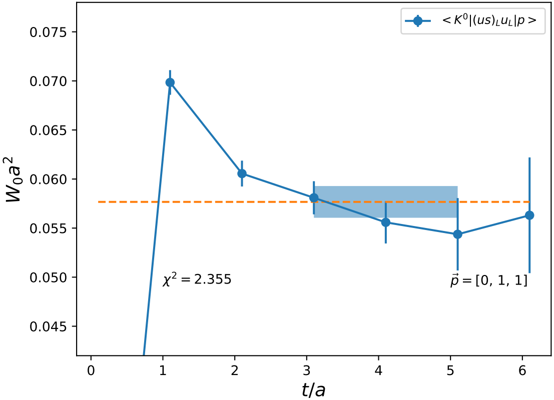

Figure 10: decay form factor $W_0^{LL}(p \to K^0 e^+)$ at $t_{sep} = 8$

Matrix elements

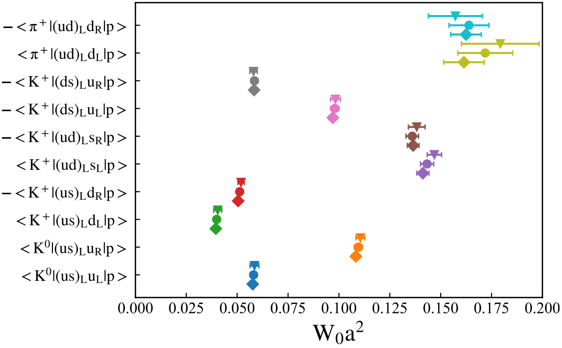

Figure 11: Decay matrix elements w/ different src-sink separation {8,9,10}

Matrix elements

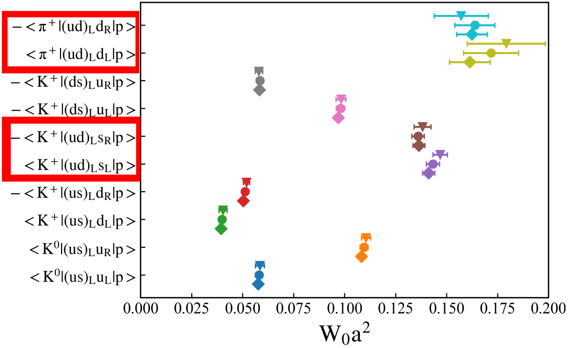

Figure 12: Decay matrix elements w/ different src-sink separation {8,9,10}

Matrix elements

Bare value, but multiplicative renormalization only

$\longrightarrow$ ratio can be compared with renormalized values

$$W_0^{norm} = \left| \frac{W_0^{\Gamma\Gamma'}(Channel)}{W_0^{\Gamma\Gamma'}(\langle K^+|(ds)_\Gamma u_{\Gamma'}|p\rangle)} \right| \tag{3}$$

Matrix elements

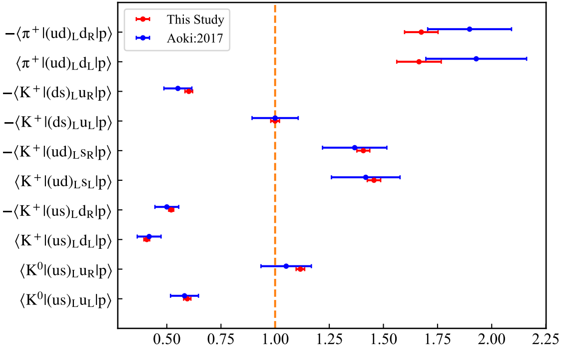

Figure 13: Comparison with earlier study, (AOKI et al., 2017)

Matrix elements

	Stat. [%] (This study)	Stat.[%] (Aoki:2017)	Chiral extrapol.[%]	a^2 [%]	Δ_Z [%]
$\langle K^0 \vert (us)_L u_L \vert p\rangle$	2.80	3.5	3.1	5.0	8.1
$\langle K^0 \vert (us)_L u_R \vert p\rangle$	1.77	2.8	2.8	5.0	8.1
$\langle K^+ \vert (us)_L d_L \vert p\rangle$	3.32	4.4	7.5	5.0	8.1
$-\langle K^+ \vert (us)_L d_R \vert p\rangle$	2.24	3.7	3.5	5.0	8.1
$\langle K^+ \vert (ud)_L s_L \vert p\rangle$	2.13	3.0	3.9	5.0	8.1
$-\langle K^+ \vert (ud)_L s_R \vert p\rangle$	2.12	3.2	1.6	5.0	8.1
$-\langle K^+ \vert (ds)_L u_L \vert p\rangle$	2.01	2.8	2.1	5.0	8.1
$-\langle K^+ \vert (ds)_L u_R \vert p\rangle$	2.96	3.6	2.7	5.0	8.1
$-\langle \pi^+ \vert (ud)_L d_R \vert p\rangle$	6.17	3.4	2.7	5.0	8.1
$\langle \pi^+ \vert (ud)_L d_R \vert p\rangle$	4.62	3.0	2.7	5.0	8.1

Table 1: Left : Comparison of statistical errors. Right: Systematic errors in chiral extrapolation, $O(a^2)$, Δ_Z ((AOKI et al., 2017))

Stony Brook University

More on correlation functions

Correlation functions show excited states signal as well

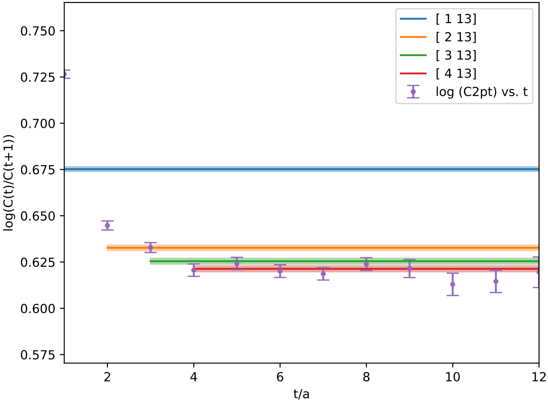

Excited states contamination

Expanding identity further,

$\mathbb{1} = \sum_{\vec{p}} |K;\vec{p}\rangle \frac{1}{2E(\vec{p})} \langle K;\vec{p}| + |K^{1st};\vec{p}\rangle \frac{1}{2E^{1st}(\vec{p})} \langle K^{1st};\vec{p}| + \dots$

Two state form of 2pt-function

$$C_K^{2pt}(t,\vec{p}) = \frac{Z_K^{gs}}{2E^{gs}(\vec{p})} e^{-E^{gs}(\vec{p})t} + \frac{Z_K^{1st}}{2E^{1st}(\vec{p})} e^{-E^{1st}(\vec{p})t}$$
$$= C_K^{2pt,gs}(t,\vec{p}) + C_K^{2pt,1st}(t,\vec{p})$$

More on correlation functions

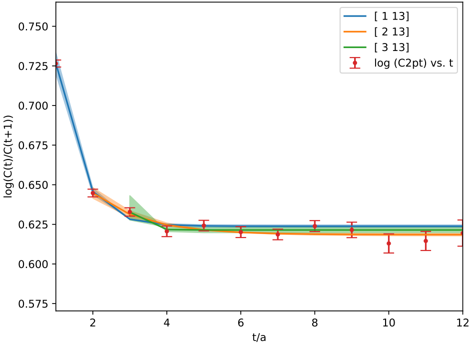

Figure 15: two-state fit to Kaon 2pt function

2pt function at early times show some excited states near source.

Excited states contamination

$$C^{3pt}(t,t') = \sum_{\vec{x},\vec{x}'} e^{i\vec{p}\cdot\vec{x}} e^{-i\vec{p}'\cdot\vec{x}'} \langle 0|J_\Pi(x')\mathcal{O}(x)\bar{J}_N(x_0)|0\rangle$$

$$= \frac{C_\Pi^{2pt,gs}(t'-t,\vec{p}')}{\sqrt{Z_\Pi^{gs}}} \frac{C_p^{2pt,gs}(t,\vec{p})}{\sqrt{Z_p^{gs}}} \times \langle \Pi^{gs}(\vec{p}')|\mathcal{O}|N^{gs}(\vec{p})\rangle$$

$$+ \frac{C_\Pi^{2pt,1st}(t'-t,\vec{p}')}{\sqrt{Z_\Pi^{1st}}} \frac{C_p^{2pt,gs}(t,\vec{p})}{\sqrt{Z_p^{gs}}} \times \langle \Pi^{1st}(\vec{p}')|\mathcal{O}|N^{gs}(\vec{p})\rangle$$

$$+ \frac{C_\Pi^{2pt,gs}(t'-t,\vec{p}')}{\sqrt{Z_\Pi^{gs}}} \frac{C_p^{2pt,1st}(t,\vec{p})}{\sqrt{Z_p^{1st}}} \times \langle \Pi^{gs}(\vec{p}')|\mathcal{O}|N^{1st}(\vec{p})\rangle$$

$$+ \frac{C_\Pi^{2pt,1st}(t'-t,\vec{p}')}{\sqrt{Z_\Pi^{1st}}} \frac{C_p^{2pt,1st}(t,\vec{p})}{\sqrt{Z_p^{1st}}} \times \langle \Pi^{1st}(\vec{p}')|\mathcal{O}|N^{1st}(\vec{p})\rangle$$

Stony Brook University

Excited states contamination

Excited states contamination

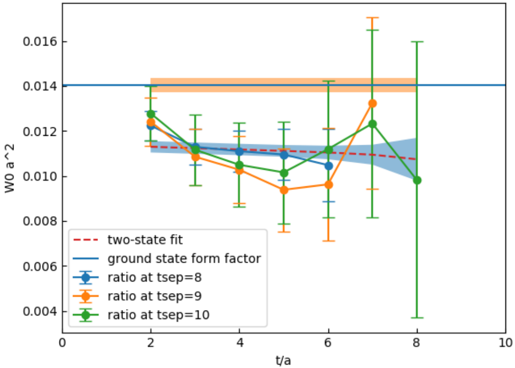

Excited states contamination

We plan to do the renormalization after we have control over excited states contamination.

(a) spacetime discretization results in the lattice regularization with cutoff scale $1/a$

(b) can employ nonperturbative renormalization

Future projects

Proton decay matrix elements can be investigated futher to see:

- Induced Nucleon Decay from Dark matter
- Vector meson channels from proton decay
- Three body decay channel from proton decay

Future projects

Induced Nucleon Decay model (DAVOUDIASL et al., 2010)

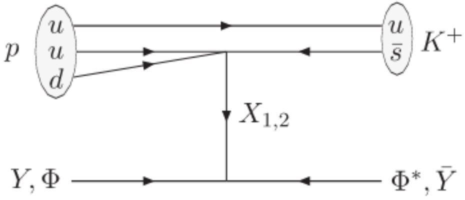

- DM can annihilate the nucleon
- $\mathcal{L}_{eff} \sim (1/\Lambda^3) u_R d_R d_R Y_R \Phi +$ h.c.
- $\langle \Pi(p') | O^{\Gamma\Gamma'}(q) | N(p,s) \rangle = P_{\Gamma'} \left[W_0^{\Gamma\Gamma'}(q^2) + \frac{m_Y}{m_N} W_1^{\Gamma\Gamma'}(q^2) \right] u_N(p,s)$

Stony Brook University

Vector meson channels

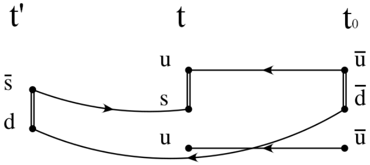

- Same computation with different Γ structures
- Different form factor decomposition

$$\langle K^{*i}(Q)\ell(p')|O_{d=6}|p(p,s)\rangle = \epsilon^i_\mu \bar{v}^c_\ell [F_1\gamma_5\gamma^\mu + F_2 i\gamma_5\sigma^{\mu\nu}Q_\nu + F_3\gamma_5 Q^\mu + F'_1\gamma^\mu + F'_2 i\sigma^{\mu\nu}Q_\nu + F'_3 Q^\mu]u_N \quad (4)$$

Three body decay

A few reasons to compute three body decay :

- Resonant to vector meson channels : $p \to K^* + \bar{\ell} \to (K\pi)\bar{\ell}$
- Decay rate ratio $(\Gamma(p \to \pi\pi e^+)/\Gamma(p \to \pi e^+))$ estimates to $\sim$ 24–150% (WISE; BLANKENBECLER; ABBOTT, 1981)
- Prime channel of next generation experiment
- Numerically cheapest among three body decay channels

Decay Mode	Water Cherenkov		Liquid Argon TPC	
	Efficiency	Background	Efficiency	Background
$p \to K^+\overline{\nu}$	19%	4	97%	1
$p \to K^0\mu^+$	10%	8	47%	< 2
$p \to K^+\mu^-\pi^+$			97%	1
$n \to K^+e^-$	10%	3	96%	< 2
$n \to e^+\pi^-$	19%	2	44%	0.8

Figure 17: DUNE proton decay efficiency

Reference

Reference

ABE, K. et al. Hyper-Kamiokande Design Report. 2018.

AOKI, S. et al. Nucleon decay matrix elements from lattice QCD. *Phys. Rev.*, D62, p. 014506, 2000.

AOKI, Y. et al. Improved lattice computation of proton decay matrix elements. *Phys. Rev.*, D96, n. 1, p. 014506, 2017.

DAVOUDIASL, H. et al. Hylogenesis: A Unified Origin for Baryonic Visible Matter and Antibaryonic Dark Matter. *Phys. Rev. Lett.*, v. 105, p. 211304, 2010.

HYPER-K. ⟨http://www.hyper-k.org/en/physics.html⟩. Accessed: 2019-01-14.

WISE, M. B.; BLANKENBECLER, R.; ABBOTT, L. F. Three-body Decays of the Proton. *Phys. Rev.*, D23, p. 1591,

Backup

Backup slides